PARTICLE SIZE IN SOLID ROCKET MOTOR PLUME: NEW EXPERIMENTAL METHOD

F. Maggi, S. Carlotti, L. Galfetti *

Politecnico di Milano
Dept. of Aerospace Science and Technology
34 via La Masa, 20156 Milano, Italy

M. Liljedahl

Swedish Defence Research Agency (FOI)
SE-147 Tumba, Sweden

D. Saile , A. Gülhan

German Aerospace Center (DLR)
Supersonic and Hypersonic Technologies Dept.
Linder Hohe, Cologne, Germany

T. Langener, J. Van den Eynde

European Space Agency (ESA/ESTEC)
Flight Vehicle & Aerothermodynamics
Engineering Section (TEC-MPA)
Keplerlaan, Noordwijk, The Netherlands

ABSTRACT

Solid propellant rocket boosters release metal oxide particulate in the atmosphere, as a result of the combustion of the aluminum powder contained in the energetic material. The characterization of these particles is still an open question regarding the environmental impact of space launch activities. For this reason an innovative collection technique was conceived in the frame of the EMAP (Experimental Modelling of Alumina Particulate in Solid Booster) project, an activity financed by the European Space Agency. The method consists in an intrusive probe capable of quenching and capturing the particles exiting from the nozzle, thus enabling size measurement, chemical characterization, and morphology observation. This paper presents an overview of the activity and reports some preliminary results obtained from the initial particle size characterization.

Index Terms— aluminum oxide, nozzle, environmental impact, probe, collection

1. INTRODUCTION

Space launch operations are not exempt from environmental impact. An AGARD meeting in 1995 tried to assess if relevant pollution was introduced by rockets. The conclusions suggested that the impact was minimal, compared to other manned activities [1]. The workshop underlined that only localized effects were possible, promptly removed by atmospheric recirculation. Despite some open issues were unresolved, such as heterogeneous reaction among the particulate and the chemicals exhausted in the plume under stratospheric conditions, a reassuring scenario was presented. According to the launch baseline activity of that decade (some tens of large rockets per year), even similar at the time being, global hazards for climate change were not foreseen. Nowadays, the perspectives of a strengthening space economy is rising the concerns about real environmental effects. Among the others, release altitude and lifetime of fine particulate have been considered important aspects of rocket effects on the atmosphere [2, 3, 4]. In this respect, the EMAP project is an international joint effort financed by ESA involving research groups from DLR (Germany), FOI (Sweden), and POLIMI (Italy) and aiming at better investigating the features of the particles exhausted from rocket motors.

Typically, boosters of heavy launchers are powered by metalized solid propellants, containing micrometric aluminum powders. From the ideal viewpoint, the addition of Al improves gravimetric and volumetric specific impulse. The adiabatic flame temperature increases along with the molar mass of the exhaust products. Thermodynamics predicts that a typical composition made by $68\,\%$ of ammonium perchlorate, $18\,\%$ of aluminum, and $14\,\%$ of polybutadiene binder burning at $7\,\mathrm{MPa}$ produces a temperature of $3404\,\mathrm{K}$ in the combustion chamber. After an expansion ratio of 40 about $315\,\mathrm{s}$ of vacuum specific impulse is granted, exhausting $34\,\%$ by mass of condensed aluminum oxide (NASA CEA [5]). Actually, the real performance is affected by the presence of agglomerates into the nozzle flow and predictions should account for losses mainly due to two-phase flow and, in case of compact motors, incomplete combustion [6, 7].

*The authors acknowledge the financial support of the European Space Agency through the contract No. 4000114698/15/Nl/SFe.

1.1. Condensed combustion products

The combustion of aluminum particles inside a rocket can be conceptually divided into three steps: the aggregation-to-agglomeration process occurring at the burning surface, the core flow evolution, and the nozzle expansion. The first step consists in the grouping of particles into irregular heaps and, after inflammation, their release into the core flow as drops [8]. This part is influenced by the composition, the burning pressure, and the microstructure of the propellant [9, 10]. The second step consists in the combustion of the residual metal inside the flow of the rocket. The aluminum is oxidized mainly by reaction with oxygen, water, and carbon dioxide [11]. Recent studies predict possible droplet break-up once they are released from the burning surface, depending on local core flow conditions [12]. Complete combustion is obtained if enough residence time is granted to the agglomerate. The condensed combustion products (CCP) consist in a multimodal particle distribution covering sub-micrometric range (smoke oxide particles, SOP), up to some tens of microns (agglomerates) [13].The third step is the evolution of the metal droplets within the accelerated flow of the nozzle. A relative velocity is generated between gas and particles. The Weber number of particles rapidly increases in the proximity of the nozzle throat, reaching the critical limit for breakup [14, 15]. Turbulent mixing and differential velocity between particles of different size can also generate the conditions for growth due to collision in the convergent part [16, 17]. Hermsen presented a global database of particles exiting from the nozzles [18]. Results of this kind were reported also in a NASA handbook specialized in solid propellant performance prediction [19] demonstrating that exiting CCP should feature a volume mean diameter lower than about $20\,\mu\mathrm{m}$. The size is dependent on expansion nozzle properties and, in part, on composition.

1.2. Collection of plume CCP

The simplest method for characterization of plume content consisted of using impinging surfaces, such as microscope slides, exposed in the vicinity of a rocket motor [20]. Optical post-processing was conducted through microscopic counting. The authors acknowledged that the mean mass of CCPs was mainly dictated by large particles, losing part of the fine fraction. Moreover, impact with the surface could alter the morphology of the collected material. In the attempt to have more representative collection, Sehgal fired a rocket fully enclosed in a tank, promoting the post-fire collection of all the exhaust products [21]. The operating rocket motor pressure was adjusted by varying the nozzle throat diameter. Dobbins and Strand extended the test methodology by changing tank size, nozzle, and aluminum content from $2\,\%$ to $20\,\%$ [22]. Scattering of collected data made the authors conclude that effects were minor under the investigated conditions.

Direct collection from the plume was performed by a probe developed by Burns [23]. The probe featured a swinging motion through the rocket exhaust thanks to a hydraulic actuator. The probe chamber was initially under vacuum and a check valve was opened by the exhaust dynamic pressure. The AFRPL (Air Force Rocket Propulsion Laboratory) developed a subsonic sampling probe consisting in a torpedo-shaped tube, placed downstream the nozzle of a BATES motor [24]. The collection technique evolved in a supersonic version by Kessel [25]. The flow inside the inner channel was supersonic and avoided front shock. The particles were slowed down and impacted against a Millipore sub-micrometric filter at the exit of the apparatus. The capturing of particles was handled differently by Carns and co-authors [26]. They described in a patent a system to remove solid particles from the exhaust flow of solid rocket motors (scrubber) before releasing the gas into the atmosphere. Even though it was not specifically designed to collect CCPs, particle separation was attained.

2. ROCKET PROBE COLLECTOR

A probe was conceived to collect a representative population of particles directly from the plume of a solid propellant rocket motor. For a matter of reference the following inlet conditions were assumed: Mach number 3.23, static temperature $2226\,\mathrm{K}$, static pressure $0.053\,\mathrm{MPa}$. Direct collection was preferred to minimize post-combustion effects and selective loss of sample population when interacting with the external flow. The conceptual block schematics is reported in Fig. 1. The operational version of the probe merges the concept of the supersonic capturing methodology by Kessel [25] and the technique for particle segregation of the scrubber by Carns and co-authors [26]. A simplified scheme is reported in Figure 2. A straight inlet duct captures the flow. After that, a secondary inert gas, nitrogen, is radially injected enabling a progressive deceleration and cooling of the primary flow in such a way that any strong shock is avoided or delayed until the particles reach a temperature lower than the alumina melting one. After a straight channel, which ensures the time and space for complete mixing, the flow enters into a conical divergent channel where the supersonic-to-subsonic transition, if not yet occurred, is caused by a shock wave. The presence and position of the shock is defined by the global design which ensures a passive control of the downstream pressure. A more in-depth discussion concerning the design methodology can be found in Carlotti et al. [27].

Finally, the collection of the particles is performed by a conical liquid spray acting in counterflow with respect to the ingested gas. The spray impacts the particles and the suspension is retained in an annular region. The liquid is then removed after each test. A scheme of the capturing device is reported in Figure 3. The reader should note that the current configuration is conceived for a rocket motor firing upside-down and can be easily modified to satisfy other requirements.

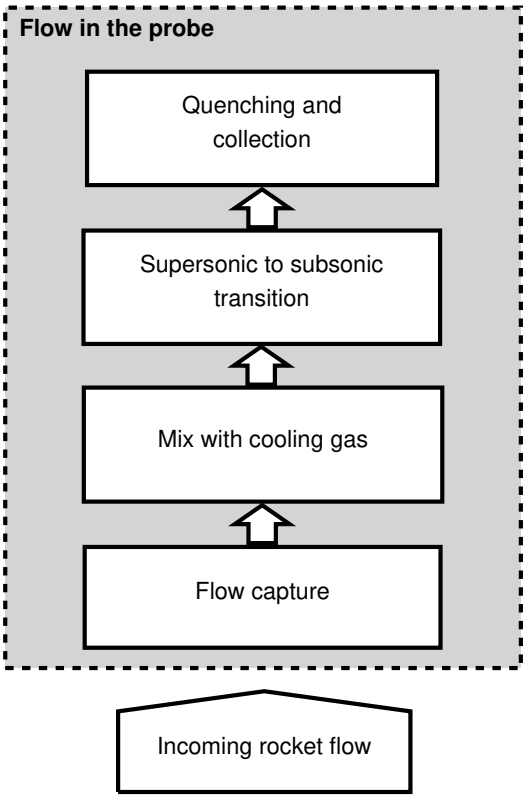

Fig. 1: Conceptual blocks of the probe

The internal structure of the collection system is reported in Figure 4. The flow is captured by the tip where a straight channel discharges in the mixing duct. Cooling nitrogen is introduced radially. Temperature and Mach number progressively lower. Axial symmetric simulations have shown a series of weak oblique shocks interacting with the viscous boundary layer, without choking the channel. The flow finally enters a divergent duct. The position of the supersonic-to-subsonic transition depends on the back pressure generated in the collection camber and regulated by the diameter of the dump ducts. The spray of the quenching liquid is operated in this last segment. The correct functioning of the probe is granted by pressure level inside the collection chamber, in turn influenced by the mass flow rates carried by nitrogen injection, inlet flow, and possible evaporation rate of the quenching liquid. The influence of these parameters on the probe behavior has been analyzed through a sensitivity and uncertainty analysis by Carlotti et al. [28]. Results highlighted the robustness of the concept since most of the effects caused by the variability of inputs canceled each other and resulted in a wide operational range. An example of the sensitivity of the mass ratio (MR) between nitrogen and inlet flow rate is reported in Figure 5. The computation is performed with quasi-1D solver based on viscous compressible equations in the form proposed by Shapiro [29]. This simulation cannot capture completely the intrinsic two-dimensional nature of the oblique shocks but provides a rapid method to obtain an approximation of the flow behavior, quickly solved by a simple ODE algorithm.

The body of the probe is made of stainless steel and is directly exposed to the flow. The thermal design was conceived to sustain the flow temperature for about $0.5\,\mathrm{s}$ to $1\,\mathrm{s}$. Passive thermal protections are applied to the body. A layer of aramidic fiber is glued to the metal directly facing the hot flow. High temperature refractory paste is applied to nitrogen pipes and connections. High temperature silicon sealing is used to fill the gaps between the components. In addition, a movable tungsten shutter is operated in front of the probe as a protective thermal shield. The tip is produced with compact graphite, aiming at resisting to high thermal stresses.

The RPC was implemented at the VMK wind tunnel located at the German Aerospace Center (DLR) in Cologne. The VMK is a vertical blow-down type wind tunnel facility with an open section for tests in the subsonic and supersonic flow regime [30]. The combination of having the wind tunnel nozzle vertically aligned and featuring an open test section offers wide space for highly instrumented experiments such as the ones in the frame of the ESA-EMAP project. The wind tunnel model mimics the base region of a space launcher. To simulate a flight-realistic exhaust plume, a solid rocket motor is integrated in the base model. The rocket motor expels the hot jet in the upward direction through a nozzle. Simultaneously, the wind tunnel provides an ambient flow at Mach 0.8. In other words, a co-flow between a cold ambient flow and a hot solid propellant exhaust jet is investigated. The probe was installed along with a set of other optical diagnostics for the simultaneous characterization of rocket plume. A complete overview of the project and more details about the measurement systems are provided in [31].

3. RESULTS

3.1. Cold flow collection tests

Cold flow experiments have been implemented at a representative Mach number to verify the capturing concept. The VMK was operated with a contour nozzle granting a Mach number equal to 3 at the exit section. The flow expanded from ambient temperature and different total pressures. Two phase flow was produced through an in-house seeder.

The RPC did not use thermal protections nor thermal resistant tip. The shield was not adopted. For simplicity the quenching liquid was water. The required nitrogen mass flow rate (set for these test to $0.042\,\mathrm{kg\,s^{-1}}$, about 10 times the ingested supersonic mass flow) was controlled by a Bronkhorst flow meter (Bronkhorst IN-Flow F-116BI-IIU-90-V). A relay switch circuit controlled by dedicated Arduino board dictated the opening and closure of an electrovalve which assured the correct functioning of the injector for 1 second. Eventual pressure transducer could be inserted both in the

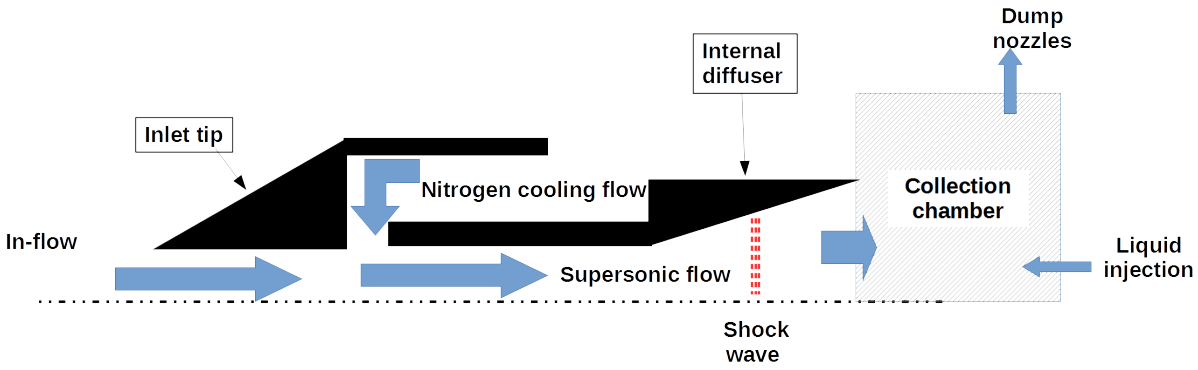

Fig. 2: Logical scheme of the supersonic rocket particle collector (RPC) [27].

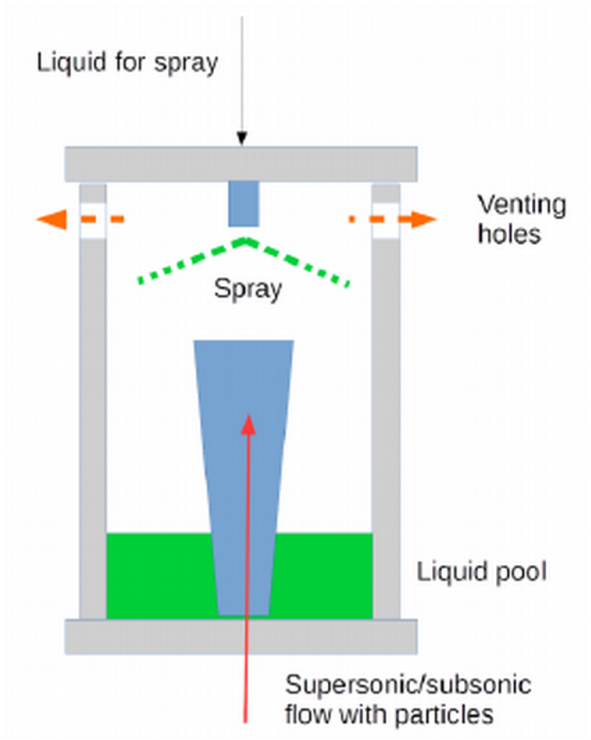

Fig. 3: Scheme of the particle capturing method

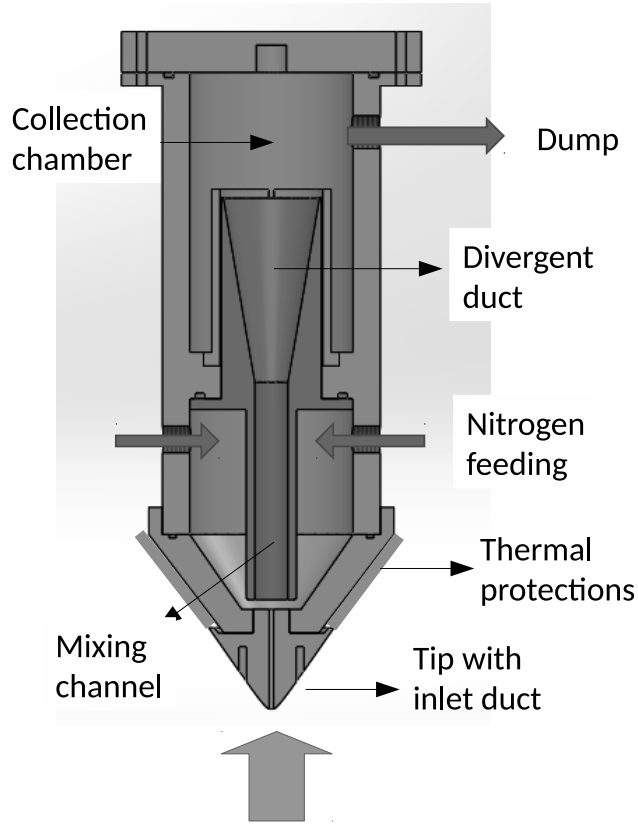

Fig. 4: Internal scheme of the probe

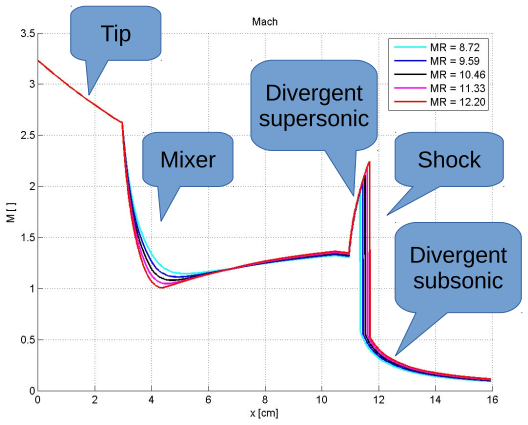

Fig. 5: Mach number inside the probe (quasi 1D Shapiro method). MR: nitrogen-to-inlet mass flow ratio

nitrogen stagnation chamber and in the collection chamber for pressure monitoring. Non-symmetrical nitrogen injection caused a spinning flow inside the probe capable of enhancing the mixing with the ingested mass flow rate, as characterized by oil flow visualizations.

The flow was seeded with sieved inert micrometric particles of magnesium oxide. The particle size distribution was obtained using laser diffraction methodology with Malvern Mastersizer 2000 instrument with water dispersion. Table 1 summarizes the tests comparing both the volume-mean (D_{43}) and the surface-mean (D_{32}) diameter of particles before and after collection and treatment procedure for wind tunnel total pressure of 25 bar. Values are substantially coincident.

Table 1: Validation of collection method: original and collected inert particle diameters

	D_{32}, µm	D_{43}, µm
original	5.693	17.03
collected	5.572	16.99

3.2. Hot flow preliminary results

The hot flow test campaign consisted in the firing of a set of rocket motors propelled with grains produced by FOI. The propellants were based on HTPB, AP, and aluminum (aluminum oxide in case of inert tests). The propellant had end-burning configuration with diameter of 86 mm and a length of 107 mm. Different nozzle expansion ratios and throat diameters permitted the investigation of a wide range of conditions. Details of the test implementation are given in a parallel paper by Saile and co-authors [31]. The preliminary results reported in this paper are referred to a propellant made of 14 % of HTPB, 56.1 % of coarse ammonium perchlorate, 24.4 % of jet-milled fine ammonium perchlorate, 5 % of Alpoco type II aluminum powder (nominal diameter 12 µm to 18 µm), and 0.5 % of iron oxide catalyst. The NCO-OH ratio was 0.8.

The tungsten thermal shield was operated by an arm commanded by the control loop of the wind tunnel and triggered by the pressure level of the rocket motor. The main control system identified the pressure rise inside the combustion chamber. After a pre-determined delay excluding the ignition transient, the spray was triggered and, after about 200 ms the opening command was sent to the shield. The closing of the shield was sent after 0.5 s to 0.7 s. The effective exposure time was influenced by the inertia of the moving arm but this value was not critical for the measurement. A final spray was finally released without inlet flow to clean up the collection volume. The timing scheme of the RPC test is depicted in Figure 6a while Figure 6b shows the real pressure signals.

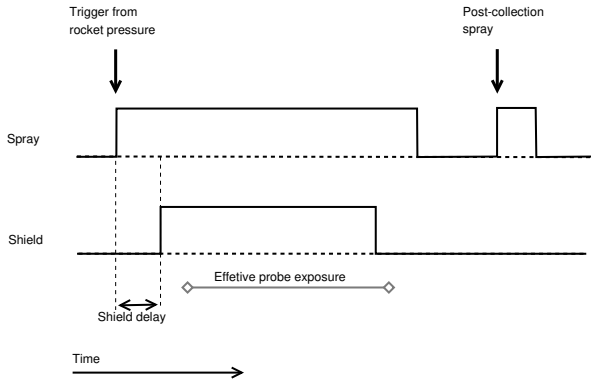

(a) Timing scheme

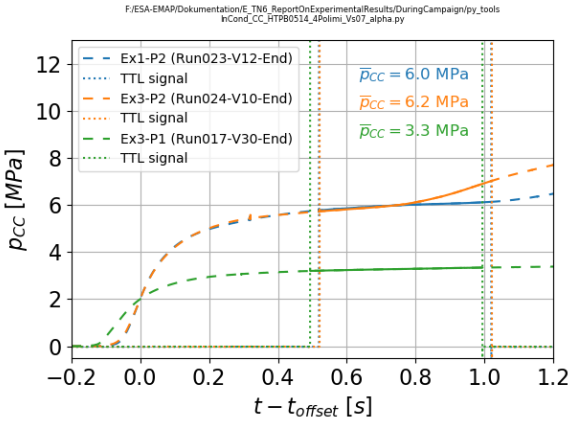

(b) Pressure traces with triggers highlighted

Fig. 6: Timing of the probe during hot flow tests

The exposure to the hot flow demonstrated the substantial validity of critical components, such as the inlet tip and most of the passive thermal protections. A detailed description of this aspect was given in a previous conference paper by Maggi and co-authors [32]. The hot flow collection was performed quenching the particles in a chlorine-based hydrocarbon liq-

uid. Then, separation between solid and liquid phase was conducted. Finally, oven drying process ensured the preservation of the collected material, till final laboratory tests. The preliminary results for Runs 17, 23, and 24 are here reported (three measurements per each collected sample). Condensed data and distributions are reported in Figures 7, 8, and 9. The symbols $d(0.1)$, $d(0.5)$, and $d(0.9)$ are used to mark the 10th, 50th, and 90th percentiles respectively. Surface-mean and volume-mean diameters are marked as D_{32} and D_{43}. Each run is assocuated to a mean rocket operating pressure, computed as the average of the recorded value during the effective probe exposure.

3.2.1. *Run 17*

- Mean chamber pressure: 3.3 MPa
- Expansion ratio: 14
- Nominal exit Mach No.: 3.23

Id.	d(0.1)	d(0.5)	d(0.9)	D_{32}	D_{43}
Run 17 a	1.008	3.362	26.37	1.733	8.237
Run 17 b	1.005	5.368	41.32	1.863	15.00
Run 17 c	0.991	3.737	32.71	1.743	11.07

(a) Particle size data

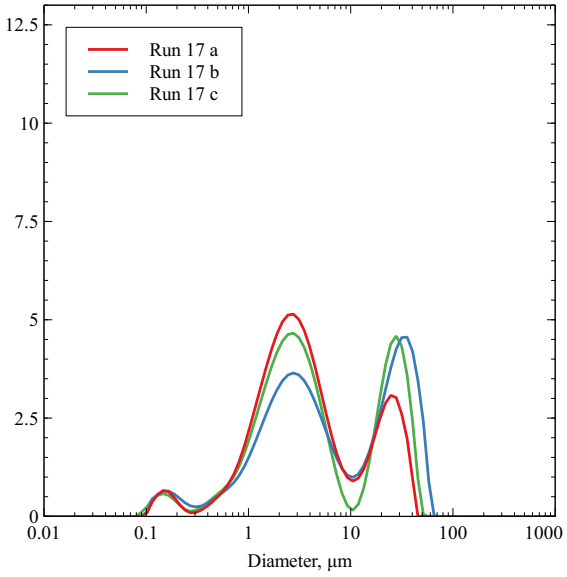

(b) Particle size distributions

Fig. 7: Analysis of CCP from Run 17 (three measurements of collected sample)

3.2.2. *Run 23*

- Effective chamber pressure: 6.0 MPa
- Expansion ratio: 1.0
- Nominal exit Mach No.: 1.0

Id.	d(0.1)	d(0.5)	d(0.9)	D_{32}	D_{43}
Run 23 a	3.330	30.46	49.01	5.455	29.17
Run 23 b	1.933	26.66	51.13	3.250	25.78
Run 23 c	3.101	38.79	73.27	7.927	38.65

(a) Particle size data

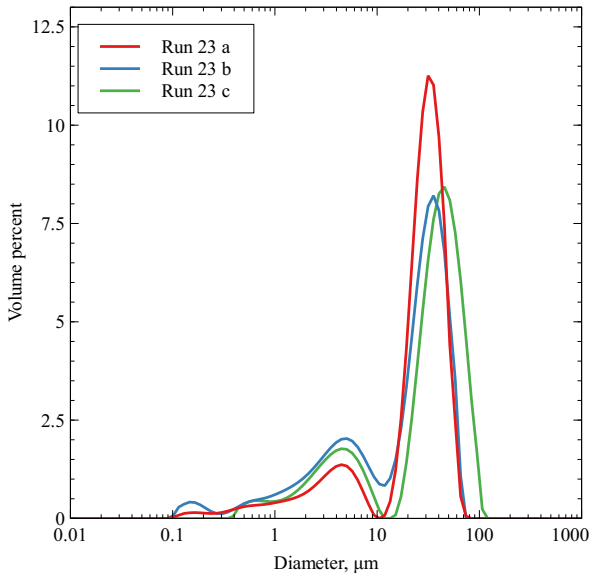

(b) Particle size distributions

Fig. 8: Analysis of CCP from Run 23 (three measurements of collected sample)

3.2.3. *Run 24*

- Effective chamber pressure: 6.2 MPa
- Expansion ratio: 14
- Nominal exit Mach No.: 3.2

4. DISCUSSION

Particle size distributions collected by the three cases feature quite different properties. Both Run 17 and 23 show a marked multimodal behavior. The coarsest mode can be identified in the range 10 µm to 70 µm. In addition a finer mode can be observed between 1 µm to 10 µm. Sub-micrometric particles are present as well, in some cases as an independent mode,

Id.	d(0.1)	d(0.5)	d(0.9)	D_{32}	D_{43}
Run 24 a	0.118	3.407	14.166	0.484	5.543
Run 24 b	1.258	4.105	21.409	2.866	7.574
Run 24 c	1.112	3.347	11.214	2.431	5.043

(a) Particle size data

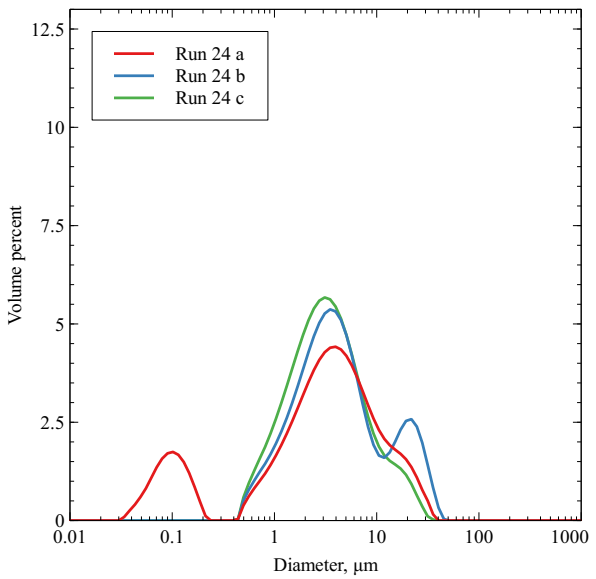

(b) Particle size distributions

Fig. 9: Analysis of CCP from Run 24 (three measurements of collected sample)

in some other case as the finer tail of the particles belonging to the micron range. Run 24 shows a more compact distribution, without distinctive behavior. When runs 17 and 23 are compared, the coarsest mode is visibly more evident in the second one. The reason can be identified in the different expansion ratio. Run 23 does not have a divergent presumably causing lower fragmentation of the coarse fraction. Run 17 takes advantage of stronger fragmentation due to high expansion ratio but low combustion pressure does not play in favor to the combustion of the metal. The comparison with Run 24 shows that the coarsest peak was collapsed with the main one. This variation was initially attributed to the high combustion pressure but the matter is still open. Mean parameters reported in the tables also follow the same trends. It should be added that reproducible sampling of the material is difficult to obtain because of the strong multiphase nature of the liquid measurement. Scanning Electron Microscope with Energy Dispersive X-ray (SEM-EDX) visualizations are underway to visually inspect samples and understand the type and shape as well as the chemical nature of the collected items.

5. CONCLUSION

A supersonic probe for the collection of metal oxide particles from the plume of a rocket motor has been developed. The paper described the working principle and the main design aspects. A cold flow test campaign proved that the working principle could capture micrometric particles suspended in supersonic flow at relevant Mach number. Hot flow tests now are concluded. Preliminary analyses are based on laser scattering analyses and show multimodal distributions with mean diameters comparable to the data available from the literature.

A set of microscopic visualizations are currently underway with the scope to confirm the data obtained from granulometric measurement along with the chemical composition of the collected particles. So far the probe and the operating procedures developed for the test campaign demonstrated to obtain the expected results. The principle can be extended to operate with larger rockets after adaptation of the thermal management.

6. REFERENCES

[1] Research and Technology Organisation (NATO), *Environmental Aspects of Rocket and Gun Propulsion*, vol. AGARD-CP-559 of *AGARD Conference Proceedings*, 1995.

[2] M. Ross, M. Mills, and D. Toohey, "Potential climate impact of black carbon emitted by rockets," *Geophysical Research Letters*, vol. 37, no. 24, 2010.

[3] S. Solomon, "Stratospheric Ozone depletion: a review of concepts and history," *Reviews of Geophysics*, vol. 37, no. 3, pp. 275–316, 1999.

[4] C. W. Hawks, "Environmental effects of solid rocket propellants, perceptions and realities," in *Environmental Aspects of Rocket and Gun Propellants*. NATO, 1995, vol. AGARD-CP-559 of *AGARD Conference Proceedings*.

[5] S. Gordon and B. S. McBride, "Computer program for calculation of complex chemical equilibrium compositions and applications," Tech. Rep. RP-1311, NASA Reference Publication, 1994.

[6] D. Reydellet, "Performance of rocket motors with metallized propellants," Advisory Report AR-230, AGARD, 1986.

[7] F. Maggi, A. Bandera, L. Galfetti, L. T. DeLuca, and T. L. Jackson, "Efficient solid rocket propulsion for access to space," *Acta Astronautica*, vol. 66, no. 11-12, pp. 1563–1573, 2010.

[8] E. W. Price, "Combustion of metallized propellants," in *Fundamental of Solid Propellant Combustion*, K. K. Kuo and M. Summerfield, Eds., vol. 90 of *Progress in Astronautics and Aeronautics Series*, pp. 479–513. AIAA, New York, NY, USA, 1984.

[9] L. DeLuca, L. Galfetti, G. Colombo, F. Maggi, A. Bandera, V. A. Babuk, and V. P. Sinditskii, "Microstructure effects in aluminized solid rocket propellants," vol. 26, no. 4, pp. 724–733, 2010.

[10] F. Maggi, L. T. DeLuca, and A. Bandera, "Pocket model for aluminum agglomeration based on propellant microstructure," *AIAA Journal*, vol. 53, no. 11, pp. 3395–3403, 2015.

[11] M. W. Beckstead, "A summary of aluminum combustion," RTO-EN 023, NATO, 2002.

[12] F. Maggi, S. Dossi, and L. T. DeLuca, "Combustion of metal agglomerates in a solid rocket core flow," *Acta Astronautica*, vol. 92, no. 0, pp. 163–171, 2012.

[13] V. A. Babuk, "Problems in studying formation of smoke oxide particles in combustion of aluminized solid propellants," *Combustion, Explosion, and Shock Waves*, vol. 43, no. 1, pp. 38–45, 2007.

[14] L. H. Caveny and A. Gany, "Breakup of Al/Al_2O_3 agglomerates in accelerating flowfields," *AIAA Journal*, vol. 17, no. 12, pp. 1368–1371, Dec 1979.

[15] A. Gany, L. H. Caveny, and M. Summerfield, "Aluminized solid propellants burning in a rocket motor flowfield," *AIAA Journal*, vol. 16, no. 7, pp. 736–739, 1978.

[16] F. E. Marble, "Droplet agglomeration in rocket nozzles caused by particle slip and collision," *Astronautica Acta*, vol. 13, no. 2, pp. 159–166, 1967.

[17] C. T. Crowe and P. G. Willoughby, "A study of particle growth in a rocket nozzle.," *AIAA Journal*, vol. 5, no. 7, pp. 1300–1304, 1967.

[18] R. W. Hermsen, "Aluminum oxide particle size for solid rocket motor performance prediction," *Journal of Spacecraft and Rockets*, vol. 18, no. 6, pp. 483–490, 1981.

[19] AA.VV., "Solid rocket motor performance analysis and prediction," Tech. Rep. SP-8039, NASA, 1971.

[20] B. Brown and K. P. McArty, "Particle size of condensed oxides from combustion of metalized solid propellants," in *Symposium (International) on Combustion*. Elsevier, 1961, vol. 8, pp. 814–823.

[21] R. Sehgal, "An experimental investigation of a gas-particle system.," Tech. Rep. DTIC Accession Number AD0274314, Jet Propulsion Laboratory, 1962.

[22] R. A. Dobbins and L. D. Strand, "A comparison of two methods of measuring particle size of Al_2O_3 produced by a small rocket motor," *AIAA Journal*, vol. 8, pp. 1544–1550, 1970.

[23] E. A. Burns, "Analysis of MINUTEMAN exhaust products," Tech. Rep. DTIC Accession Number AD 432233, Aerojet General Corporation, 1962.

[24] J. A. Misener et al., "Exhaust plume measurements fo 15-pound bates motors," Tech. Rep. AFRPL TR-85-013, Air Force Rocket Propulsion Laboratory, 1985.

[25] P. A. Kessel, "Rocket exhaust probe," 1987, US Patent 4,662,216.

[26] R. H. Carns et al., "Rocket motor exhaust scrubber," 2005, US Patent 6,964,699 B1.

[27] S. Carlotti, F. Maggi, A. Ferreri, L. Galfetti, R. Bisin, D. Saile, A. Gülhan, C. Groll, and T. Langener, "Development of an intrusive technique for particle collection in rockets plume," *Acta Astronautica*, vol. 158, pp. 361–374, 2019.

[28] S. Carlotti, F. Maggi, S. Dossi, R. Bisin, L. Galfetti, D. Saile, Gülhan A., C. Groll, and T. Langener, "Overview of a supersonic probe for solid propellant rocket CCP collection," *AIAA paper*, vol. 2018-4882, 2018.

[29] A. H. Shapiro, *The dynamics and thermodynamics of compressible fluid flow*, vol. 1, Roland Press Company, New York, 1953.

[30] D. Saile, D. Kirchheck, A. Gülhan, and D. Banuti, "Design of a Hot Plume Interaction Facility at DLR Cologne," in *Proceedings of the 8th European Symposium on Aerothermodynamics for Space Vehicles*, 2015, number 83419.

[31] D. Saile, V. Kühl, C. Willert, M. Liljedahl, N. Wingborg, S. Carlotti, F. Maggi, J. van den Eynde, T. Langener, and A. Gülhan, "Overview to the esa-emap project: Characterization of srm plumes with alumina particulate in subscale testing," in *International Conference on Flight Vehicles, Aerothermodynamics and Re-Entry Missions & Engineering*, 2019, Monopoli, Italy.

[32] F. Maggi, S. Carlotti, L. Galfetti, D. Saile, A. Gülhan, M. Liljedahl, J. van den Eynde, and T. Langener, "Particle size in srm plume: assessment of collection method," in *Proceedings of the 8-EUCASS*, 2019, Madrid, Spain.